Volume 1 | Number 1 | Jan 2013 | Pages 1–100

Journal of
Materials Chemistry A

Materials for energy and sustainability
www.rsc.org/materialsA

ROYAL SOCIETY
OF CHEMISTRY

Journal Name

ARTICLE TYPE

Semiconducting Liquid Crystalline Block Copolymer Containing Regioregular Poly(3-Hexylthiophene) and Nematic Poly(*n*-Hexyl Isocyanate) and its Application in Bulk Heterojunction Solar Cells

Mahesh P. Bhatt, Jia Du, Elizabeth A. Rainbolt, Taniya M.S.K. Pathiranage, Peishen Huang, James F.
5 **Reuther, Bruce M. Novak, Michael C. Biewer, and Mihaela C. Stefan***

ABSTRACT: A liquid crystalline diblock copolymer containing regioregular poly(3-hexylthiophene)
10 (P3HT) and poly(*n*-hexyl isocyanate) (PHIC) was synthesized by the combination of Grignard metathesis polymerization (GRIM) and titanium mediated coordination polymerization methods. The poly(3-hexylthiophene)-*b*-poly(*n*-hexyl isocyanate) (P3HT-*b*-PHIC) diblock copolymer used in this study contained ~10 mol% of P3HT and ~90 mol% PHIC. The diblock copolymer displayed solvatochromism in THF/water and THF/methanol mixtures. The field-effect mobilities of the synthesized block copolymer
15 were measured in bottom gate-bottom contact organic field-effect transistors (OFETs). The surface morphology of the polymer thin film was investigated in the channel region of the OFET devices by tapping mode atomic force microscopy (TMAFM). The diblock copolymer displayed nanostructured morphology in thin film and had good mobility despite the low content of semiconducting P3HT block. The diblock copolymer was also used as an additive to improve the performance of P3HT/PCBM bulk
20 heterojunction (BHJ) solar cells. Liquid crystalline characteristics of the diblock copolymer were examined by cross polarizing microscope and X-ray diffraction.

Introduction

Poly(*n*-alkyl isocyanates) are rigid-rod polymers with helical conformation in liquid as well as in solid state.[1-9] Poly(*n*-alkyl
25 isocyanates) have been studied in a variety of fields such as liquid crystals, optical switches and chiral sensing.[8, 10-12] These polymers combine steric repulsions between the side chains with double bond character of the amide groups.[13] The steric repulsion by neighbouring side chain causes the adjacent side chain to
30 rotate out of plane giving the polymer its helical structure. A wide variety of helical conformations have been proposed for poly(*n*-alkyl isocyanates) including 2_1, 5_1 and 8_3 in solution, and 8_3, 8_5 and 12_5 in thin films.[11, 14-16] Among the polyisocyanates, poly(*n*-hexyl isocyanate) (PHIC) is one of the most intensively
35 studied.[3, 9, 17-20] The well-defined PHIC can be synthesized via organotitanium mediated *living* coordination and *living* anionic polymerization techniques.[21-25] PHIC is a helical semiflexible polymer with liquid crystalline (LC) properties.[26-28] Moreover, PHIC forms a nematic liquid crystal at high concentrations in
40 non-polar solvents.[27, 29] Even though PHIC is a lyotropic liquid crystalline polymer, its solid state properties are also promising.[18] Kawaguchi reported the Langmuir–Blodgett films of PHIC with different molecular weights, indicating that PHIC can form condensed-type thin films at the air-water interface.[26, 30, 31]
45 Recently, Tanaka's group proposed the application of PHIC in electrical devices.[18] Due to the semiflexible and helical nature of

the PHIC chain, PHIC can be integrated in a block copolymer system to attain a unique structural morphology.

Regioregular poly(3-hexylthiophene) (P3HT) is a
50 comprehensively studied semiconducting polymer for its application in flexible electronic devices.[32, 33] Grignard metathesis polymerization (GRIM), reported by McCullough's group in 1999, is a commonly employed method for the synthesis of regioregular P3HT with well-defined molecular weights.[34]
55 McCullough's group reported the *livingness* of P3HT using the GRIM method which allows the synthesis of end functionalized P3HT.[35-37] End-functionalized P3HTs have been widely used to generate various block copolymers.[38-40] P3HT is a rigid rod-like polymer with a persistence length of 2.4 nm. However, P3HT
60 does not behave like a rod above a certain molecular weight.[41] Incorporation of helical liquid crystalline polymers like polyisocyanates, which have a persistence length of 20-60 nm into the P3HT block is expected to generate unique morphologies in thin films *via* supramolecular self-assembly.[2] A systematic
65 study of morphology and optoelectronic properties of liquid crystalline diblock copolymers containing semiconducting units is a relatively unexplored area of research.[42, 43] Few reports exist regarding diblock copolymers containing main chain LC polymer and a semiconducting segment.[44] However, it has been
70 demonstrated that a diblock copolymer containing side chain liquid crystalline (SCLP) units and rr-P3HT undergoes self-assembly and microphase separation.[45]

Herein we report the synthesis and the opto-electronic properties of a diblock copolymer containing liquid crystalline poly(*n*-hexyl isocyanate) (PHIC) and a semiconducting rigid rod-like P3HT. The diblock copolymer was synthesized by combining GRIM and titanium mediated coordination polymerization techniques. We emphasize that both the liquid crystalline properties and semiconducting properties were evident in the block copolymer. Due to its unique nanostructure morphology and semiconducting properties, the use of P3HT-*b*-PHIC in thin film transistors and bulk heterojunction (BHJ) solar cells was investigated.

Experimental

Materials

All commercial chemicals were purchased from Aldrich Chemical Co., Inc. and were used without further purification unless otherwise noted. All reactions were conducted under nitrogen. The polymerization glassware and syringes were dried at 120 °C for at least 24 hours before use and cooled under a nitrogen atmosphere. Tetrahydrofuran (THF) and toluene were dried over sodium/benzophenone ketyl and freshly distilled prior to use.

Synthesis of titanium alkoxide terminated P3HT

The procedures for synthesis of allyl-terminated P3HT and hydroxypropyl-terminated P3HT are given in the Supporting Information.

The hydroxypropyl terminated P3HT (40 mg, 0.003 mmol) was dissolved in 30 mL of distilled toluene. Ethanol (5 mL) was added to the polymer solution. Azeotropic distillation was performed under a nitrogen atmosphere. Distillation was stopped after collecting 15 mL of toluene into the receiving flask. Cyclopentadienyltitanium trichloride (TiCpCl$_3$) (10 mg, 0.04 mmol) was added to the reaction and stirred for 5 h at reflux under a nitrogen atmosphere. At that time a sample was taken to monitor the conversion of hydroxyl group to titanium alkoxide using ^{1}H NMR. Toluene was removed from the reaction mixture under vacuum.

Synthesis of P3HT-*b*-PHIC copolymer

The preformed titanium alkoxide terminated P3HT was transferred into the glove box and dissolved in 7 mL of freshly distilled chloroform. Hexyl isocyanate (3.23 g, 0.02 mmol) was added to the reaction mixture in the glove box. After 12 h of stirring the reaction was stopped and the reaction mixture was quenched in methanol. The polymer was filtered in a thimble and it was extracted with methanol, hexane, and chloroform using a Soxhlet extractor. The final polymer was characterized by SEC (M$_n$ = 21000 gmol^{-1}) and ^{1}H NMR. ^{1}H NMR (500 MHz, CDCl$_3$): δH 0.91 (br, 6H), 1.32 (br, 14H), 1.57-1.65 (m, 8H), 2.84 (t, 2H), 3.45-4.03 (br, 2H), 6.98 (s, 1H).

X-Ray Diffraction (XRD)

X-Ray diffraction study was performed on a RIGAKU Ultima III diffractometer. Thin film samples were radiated by Cu-Kα (λ=1.54 Å) and scanned from 1° to 40° (2θ) at 0.04 degree interval at a rate of 2 degree/min. Thin films of the copolymers were obtained by drop casting a 5.0 mg/mL polymer solution in chloroform onto clean SiO$_2$ substrates. The solvent was evaporated slowly in a Petri dish saturated with chloroform.

UV-Vis analysis

UV–Vis spectra in solution and solid state were measured using an Agilent 8453 UV–Vis spectroscopy system. For solvatochromism study, stock solutions of the precursor P3HT and the diblock copolymer (5 mg/mL in THF) were prepared. Samples were obtained by mixing 0.1 mL of stock solution and 5 mL of solvent/non-solvent. For each sample the concentration of the polymer under study was kept constant.

Structural analysis

^{1}H NMR spectra of the synthesized monomers and polymers were recorded on a Bruker 500 MHz spectrometer at 25 °C. ^{1}H NMR data are reported in parts per million as chemical shift relative to tetramethylsilane (TMS) as the internal standard. Spectra were recorded in CDCl$_3$. GC/MS was performed on an Agilent 6890-5973 GC-MS workstation. The GC column was a Hewlett-Packard fused silica capillary column cross-linked with 5% phenylmethyl siloxane. Helium was the carrier gas (1 mL/min). The following conditions were used for all GC/MS analyses: injector and detector temperature, 250 °C; initial temperature, 70 °C; temperature ramp, 10 °C/min; final temperature, 280 °C. The UV-Vis spectra of polymer solutions in chloroform solvent were carried out in 1 cm cuvettes using an Agilent 8453 UV-VIS spectrometer. Thin-films of polymer were obtained by evaporation of chloroform solvent on glass microscope slides. Molecular weights of the synthesized polymers were measured by Size Exclusion Chromatography (SEC) analysis on a Viscotek VE 3580 system equipped with ViscoGEL™ columns (GMHHR-M), connected to a refractive index (RI) detector. GPC solvent/sample module (GPCmax) was used with HPLC grade THF as the eluent and calibration was based on polystyrene standards. Running conditions for SEC analysis were: flow rate = 1.0 mL/min, injector volume = 100 μL, detector temperature = 30 °C, column temperature = 35 °C. All the polymers samples were dissolved in THF and the solutions were filtered through PTFE filters (0.45 μm) prior to injection.

Field-effect transistor fabrication and measurement of the field-effect mobilities

Field-effect mobility measurements of the synthesized polymers were performed on thin-film transistors with a common bottom-gate, bottom-contact configuration. Highly doped, n-type silicon wafers with a resistivity of 0.001-0.003 Ω cm were used as substrates. Thermal oxide (SiO$_2$) was grown 200 nm thick at 1000 °C. Chromium metal (5 nm) followed by 100 nm of gold was deposited by E-beam evaporation as source-drain metals. The source-drain pads were formed by photo-lithographically patterning the metal layer. The SiO$_2$ on the back side of the wafer was etched with buffered oxide etchant (7:1 BOE from JT Baker) to generate the common bottom-gate. The resulting transistors had a channel width of 475 μm and channel length ranging from 2 μm to 80 μm. The measured capacitance density of the SiO$_2$ dielectric was 17 nF/cm^2. After the SiO$_2$ on the backside was removed, the devices were cleaned with UV-Ozone for 7 min using a Technics Series 85 RIE etcher and stored under vacuum. This process removed any residual organics on the substrate. Prior to the polymer deposition, the substrates were cleaned with

water, acetone, hexanes, and chloroform with drying using nitrogen flow between different solvents. The devices were baked at 80 °C for 30 min in a vacuum oven. The devices were allowed to cool under vacuum. The polymer films were deposited in air

5 by drop casting 4-5 drops of 8 mg/mL of polymer solution, previously filtered through a 0.2 μm PTFE syringe filter, using a 25 μL syringe. The films were allowed to dry in a Petri dish saturated with chloroform. The devices were annealed under vacuum for 30 min at 120 °C prior to measurements. The devices

10 were again allowed to cool down to room temperature under vacuum. A Keithley 4200-SCS semiconductor characterization system was used to probe the devices. The probe station used for electrical characterization was a Cascade Microtech Model Summit Microchamber. When measuring current–voltage curves

15 and transfer curves, VG was scanned from +20 V to –100 V. All the measurements were performed at room temperature in air. For the surface treatment with octyltrichlorosilane, the devices were rinsed sequentially with water, acetone, hexanes and chloroform and placed in a glass container in a solution of silane of 8×10^{-3} M

20 in dried toluene. The sealed container was placed in a glove box at ambient temperature for 48 h. After 48 h, the device was removed from the glovebox and rinsed with toluene before baking at 80 °C for 30 min in a vacuum oven. The procedure for the polymer film deposition was the same as described above.

25 **Tapping mode atomic force microscopy (TMAFM)**

TMAFM investigation of thin film surface morphology was carried out using a Nanoscope IV-Multimode Veeco, equipped with an E-type vertical engage scanner. AFM measurement was performed on the OFET devices that were measured for the

30 estimation of field-effect mobilities. AFM images were also recorded from thin films on mica substrate. Thin films were obtained by drop-casting chloroform solution of polymers on mica substrate. The AFM images were recorded at room temperature in air using silicon cantilevers with normal spring

35 constant of 42 N/m and normal resonance frequency of 320 kHz. A typical value of AFM detector signal corresponding to a root mean square (r.m.s.) cantilever oscillation amplitude was equal to 1-2 V and the images were collected at 0.5 Hz scan frequency in 2 μm scan size. Polymer samples were prepared in chloroform

40 solutions (1 mg/mL) and deposited on to mica substrate by drop casting.

For solar cell devices, the TMAFM was carried out on the active area in between the channels of the metal. Images were obtained using silicon cantilevers with spring constant of 42 N/m and

45 resonance frequency of 300 kHz. Images were acquired at 1 Hz scan frequency. Sample scan area was 3 μm x 3 μm.

Investigation of liquid crystalline properties

A polarizing microscope (Meiji) with an Olympus digital camera was used to study the liquid crystalline properties of polymer

50 samples. The images were recorded using QCapture software. Experiments were performed for the polymer samples in liquid state. The polymer sample was dissolved in xylene (40 wt %) and a drop of the polymer solution was sandwiched in between two glass slides.

55 **Preparation of solar cell devices**

Glass substrates coated with ITO were purchased from
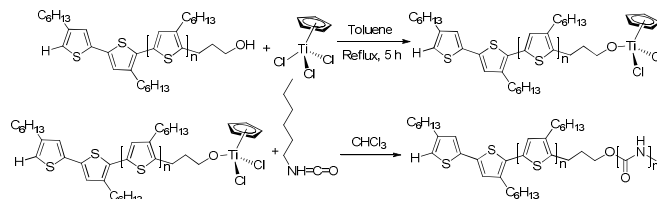
Scheme 1. Synthesis of diblock copolymer poly(3-hexylthiophene)-*b*-poly(*n*-hexyl isocyanate) (P3HT-*b*-PHIC).

60 Luminescence Technology Corp. (Taiwan) and were patterned using standard photolithography. The P3HT homopolymer was synthesized with molecular weight of 30000 g/mol by GRIM method. The substrates were cleaned by sonication for 20 minutes in acetone, methanol, toluene, and isopropyl alcohol. The

65 substrates were subjected to UV/ozone treatment for 20 minutes prior to use. After the ozone treatment, poly(3,4-ethyl-enedioxythiophene): poly(styrenesulfonate) PEDOT:PSS was spin coated on the substrates (1500 rpm, 1740 rpm s^{-1}, 90 s). The substrates were annealed at 150 °C for 10 minutes under a

70 nitrogen atmosphere. P3HT:PCBM (1:1) blends with different percentages of P3HT-*b*-PHIC were prepared in dichlorobenzene with a total blend concentration of 50 mg mL^{-1}. These blends were spin coated (2000 rpm, 1740 rpm s^{-1}, 60 s) onto the PEDOT:PSS treated substrate. The devices were annealed at 180

75 °C for 5 minutes. Films of 20 nm Ca and 100 nm Al were thermally evaporated onto the substrates at a rate of 2.75 Å s^{-1} through a shadow mask to obtain the solar cell devices. IV testing was carried out under a controlled nitrogen atmosphere using a Keithley 236, model 9160 interfaced with LabView software. The

80 solar simulator used was a THERMOORIEL equipped with a 300 W Xenon lamp; the intensity of the light was calibrated to 100 mW cm^{-2} with a NREL certified Hamamatsu silicon photodiode. The active area of the devices was 0.1 cm^2. The active layer film thickness was measured using a Veeco Dektak VIII profilometer.

85 **Results and discussion**

Synthesis and characterization of diblock copolymer

Synthesis of poly(3-hexylthiophene)-*b*-poly(*n*-hexyl isocyanate) (P3HT-*b*-PHIC) diblock copolymer is shown in Scheme 1. Allyl-terminated P3HT was synthesized by the *in situ* end capping of

90 nickel-terminated P3HT with allyl magnesium bromide (Supporting Information). Hydroboration-oxidation of the allyl-terminated P3HT generated the hydroxypropyl-terminated P3HT which was subsequently reacted with cyclopentadienyltitanium trichloride. The reaction was monitored by ^{1}H NMR and the

95 appearance of a new peak at 4.5 ppm in ^{1}H NMR spectrum indicated the formation of the titanium propoxide-terminated P3HT (Figure S3, Supporting Information). The complete disappearance of the methylene protons adjacent to the hydroxyl group at 3.78 ppm indicated the complete conversion the

100 hydroxypropyl end group to the titanium propoxide. The polymerization of hexyl isocyanate with the titanium propoxide-terminated P3HT macroinitiator was performed in a glove box.

Table 1. Molecular weights and optical properties of the P3HT precursor and P3HT-*b*-PHIC diblock copolymer

Polymer	Molecular weight (g/mol)	PDI	λ_{max}^{a} (nm)	λ_{max}^{b} (nm)
P3HT-OH precursor	12000	1.20	447	550
P3HT-*b*-PHIC	21000	1.45	250, 447	250, 550

[a]measured in THF solution; [b]measured in thin film deposited on a glass slide

The ^{1}H NMR of the diblock copolymer displayed a broad peak at 3.5 to 4 ppm due to the presence of the methylene protons adjacent to the nitrogen of PHIC. The peak corresponding to the methylene protons adjacent to the thiophene ring of the P3HT block was integrated with respect to the peak corresponding to the methylene protons adjacent to the nitrogen atom on the PHIC block. The final diblock copolymer contained 90 mol% of PHIC as determined by ^{1}H NMR (Figure S4, Supporting Information). Formation of the diblock copolymer was further confirmed by size exclusion chromatography (SEC) measurements, which displayed an increase in molecular weight of the diblock copolymer as compared to the P3HT precursor (SEC traces are shown in Figure S5, Supporting Information).

UV-Vis analysis

UV-Vis analysis of the diblock copolymer was performed in solution as well as on thin films and it was compared with P3HT-OH precursor. The UV-Vis spectrum of the diblock copolymer in THF displayed an absorption maximum at 447 nm which was attributed to the P3HT and an absorption maximum at 250 nm which was due to the organization of helical PHIC (Figure S7, Supporting Information). The thin film UV-Vis spectra of the precursor P3HT and the diblock copolymer displayed similar features except that the diblock copolymer showed a peak at 250 nm corresponding to PHIC unit (Figure S8, supporting information). The similarities in the UV-Vis spectra of the precursor P3HT and the diblock copolymer, both in solution and solid state, indicated that the PHIC block did not drastically affect the effective conjugation length of the P3HT.

A solvatochromism study was performed for the diblock copolymer and the precursor P3HT using THF/water and THF/methanol mixtures at the same concentration of polymer in solution. Water and methanol were chosen because they are non-solvents for P3HT. A red shift in UV-Vis spectra for both the precursor polymer and diblock copolymer was observed upon the addition of 10 % of non-solvent. The solvatochromism experiments were carried out up to but not including the point when the polymer precipitated out of solution. It was noted that the P3HT precursor precipitated out of the solution for 60:40 v/v THF/methanol and 40:60 v/v THF/water mixtures (Figure 1 and Figure S6, Supporting Information). However, the P3HT-*b*-PHIC diblock copolymer showed solvatochromism up to 40:60 v/v THF/methanol and 10:90 v/v THF/water mixtures. For the diblock copolymer, the absorption maxima were red shifted as compared to the P3HT precursor (Figure 1). We speculated that upon addition of water or methanol to the diblock copolymers solutions in THF, micellar aggregates are formed with a core of hydrophobic poly(3-hexylthiophene) and a shell of poly(*n*-hexyl
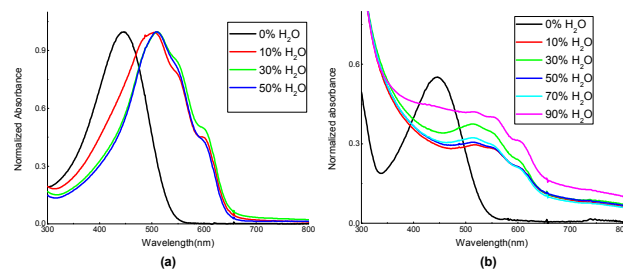

Figure 1. Solvatochromism studies with THF/water mixture; (a) P3HT and (b) P3HT-*b*-PHIC diblock copolymer

isocyanate). This result is consistent with our previous reports.[44, 47] In the THF/water mixtures, the precursor P3HT displayed the highest absorption maximum at 545 nm with π-π* transition at 600 nm when the THF/water was 50:50 v/v (Table S1, Supporting Information). At the same ratio of the solvents, the diblock copolymer showed the highest absorption maximum at 555 nm with the π-π* transition at 610 nm. However, the diblock copolymer showed highest absorption maximum of 561 nm with the π-π* transition at 612 nm when THF/water mixture was 10:90 v/v. The precursor P3HT and the diblock copolymer displayed a similar trend for THF/methanol mixtures (Figure S6 and Table S2, Supporting Information).

Field-effect mobility

The field-effect mobilities of the polymer were measured in bottom-gate bottom-contact device configuration. A plot of $I_{DS}^{1/2}$ vs. V_{GS} was obtained in the saturation regime and the field-effect mobility was calculated using following equation:

$$\mu = \frac{2L}{WC_i} \frac{I_{DS}}{(V_{GS} - V_T)^2}$$

where I_{DS} is the source-drain current, W is the channel width, L is the channel length, C_i is the capacitance of the dielectric, V_{GS} is the gate voltage and V_T is the threshold voltage.

The field-effect mobility data were consistently measured from the channel length of 20 μm in the bottom gate-bottom contact OFET devices. The data were obtained from an untreated device and from the device treated with 8×10^{-3} M of octyltrichlorosilane. The average field-effect mobility measured for an untreated device was 1.8×10^{-4} cm²/Vs with highest value of 3.2×10^{-4} cm²/Vs (Table 2 and Figure 2). However, the diblock copolymer displayed the average field-effect mobility of 1.1×10^{-3} cm²/Vs on a device treated with octyltrichlorosilane (OTS). The highest value measured for the OTS treated device was 2.1×10^{-3} cm²/Vs (Table 2 and Figure 3).

The field-effect mobilities reported for various P3HT block copolymers ranged from 10^{-2} to 10^{-5} cm²/Vs.[38, 46-49] However, those copolymers had a semiconducting block content exceeding 10 mol%. We also reported the synthesis and electronic properties of a P3HT diblock copolymer containing poly(γ-benzyl-L-glutamate).[42,44] The diblock copolymer contained ~57 mol% of semiconducting polymer segment and displayed a mobility of ~ 6×10^{-4} cm²/Vs in thin film transistors. Again, we emphasize here that the investigated P3HT-*b*-PHIC diblock copolymer contained only 10 mol% of the semiconducting block
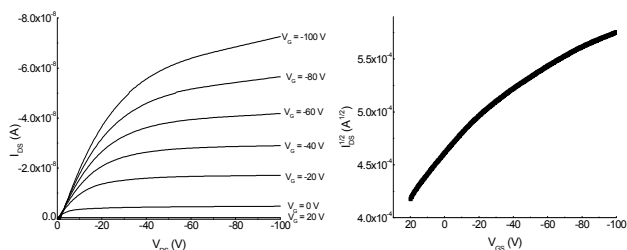
Figure 2. Current-voltage characteristics of poly(3-hexylthiophene)-*b*-poly(*n*-hexyl isocyanate) on an untreated device, output curves at different gate voltages (left); transfer curve at V_{DS}=-100 V (W = 475 μm, L = 20 μm) (right).

Table 2. Field-effect mobilities of poly(3-hexylthiophene)-*b*-poly(*n*-hexylisocyanate) (P3HT-*b*-PHIC) measured in OFET

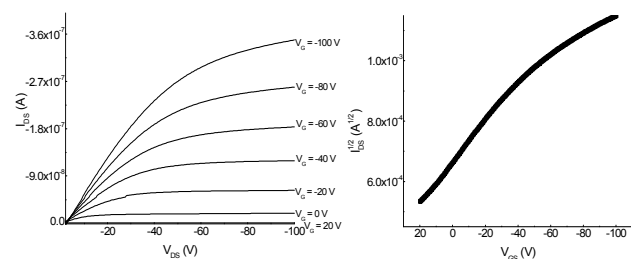| Device	Mobility(cm^2/Vs)	I_{on}/I_{off}	$V_T(V)$	Average mobility (cm^2/Vs)
Untreated	3.2×10^{-4}	4.0×10^1	19.1	
	1.5×10^{-4}	1.9×10^1	18.3	1.8×10^{-4}
	8.2×10^{-5}	7.0×10^1	23.5	
OTS treated	2.1×10^{-3}	2.3×10^1	17.4	
	7.5×10^{-4}	6.4×10^1	30.3	1.1×10^{-3}
	6.1×10^{-4}	4.0×10^1	9.1	

Figure 3. Current-voltage characteristics of poly(3-hexylthiophene)-*b*-poly(*n*-hexyl isocyanate) (P3HT-*b*-PHIC) on a device treated with OTS, output curves at different gate voltages (left); (b) transfer curve at V_{DS} = -100 V (W = 475 μm, L = 20 μm) (right).

and still possessed remarkable electronic properties in OFET devices. We speculated that the helical PHIC block enhanced the organization of P3HT in thin films. Moreover, the equal length side chains in both of the blocks in the rod-rod block copolymer possibly enabled the favorable structural morphology in thin films especially on surface treated device.

Surface morphology on thin film

The surface morphology of the polymers was investigated by TMAFM. The TMAFM analysis of the films was performed in the channel region of the OFET devices as well as on mica substrate. Thin films of polymers were drop-casted either on mica substrate or on OFET devices and the films were formed by the slow evaporation of the chloroform solvent in a chloroform chamber. TMAFM images were recorded for the precursor P3HT, a PHIC homopolymer, and the diblock copolymer. As expected, nanofibrillar morphology was observed for the P3HT homopolymer (Figure 4 (a) and (b)). By contrast, the PHIC homopolymer displayed a granular of morphology. However, the granular features were uniformly distributed in the image.
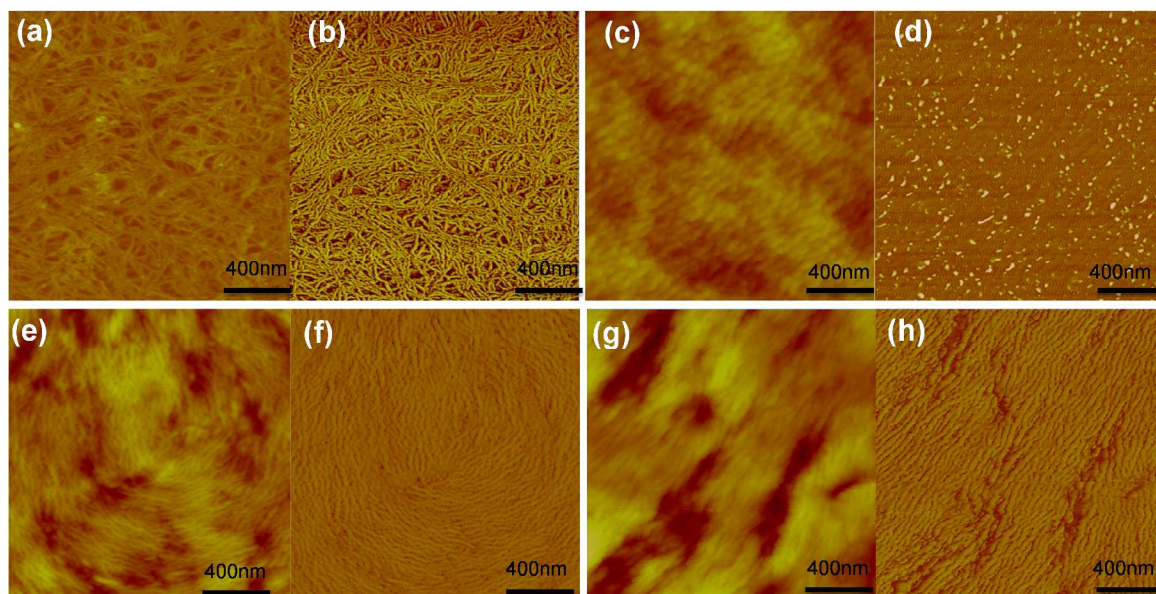

Figure 4. TMAFM images of: (a) Height and (b) phase images of P3HT on mica (0.5 mg/mL in chloroform);(c) Height and (d) phase images of PHIC on mica (8 mg/mL in chloroform); (e) Height and (f) phase images of P3HT-*b*-PHIC on mica (8 mg/mL in chloroform); (g) Height and (h) phase images of P3HT-*b*-PHIC on the channel region of OFET (8 mg/mL) (Scan size: 2×2 μm).
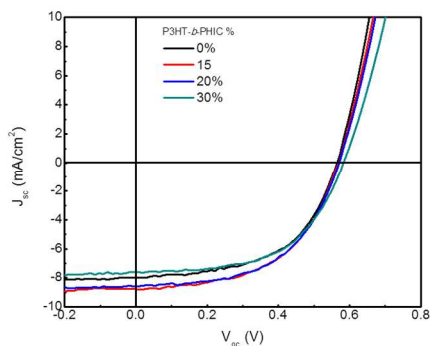
Figure 5. *J-V* curves for devices with different percentage of P3HT-*b*-PHIC

The diblock copolymer P3HT-*b*-PHIC displayed a nanoscale morphology that was different from the precursor P3HT (Figure 4). This is in contrast with the surface morphology of most of the P3HT diblock copolymers reported earlier. The surface morphologies of the P3HT diblock copolymers reported previously were dominated by nanofibrillar features of the P3HT block regardless of the block's size.[50-53] The images obtained for the P3HT-*b*-PHIC block copolymer thin film on mica were similar to the images obtained from the thin film in the OFET devices. The diblock copolymer self-assembled, leading to densely packed nanostructures. The formation of nanostructures was attributed to the self-assembly driven by the helical PHIC unit. The nanostructured morphology of the diblock copolymer thin film in the channel region of OFET devices explained the relatively good field effect mobilities which were measured for the diblock copolymers despite their very low content of P3HT semiconducting block.

Bulk heterojunction solar cell studies

The diblock copolymer was tested in BHJ solar cells with PC$_{61}$BM, and PCE lower than 0.1% was obtained. This was attributed to the large content of the insulating block. Due to the poor performance of diblock copolymer in BHJ, we decided to use the diblock copolymer in a P3HT:PCBM:P3HT-*b*-PHIC ternary blend. Adding the P3HT-*b*-PHIC was expected to modify the P3HT:PCBM microstructure and improve the performance of solar cells.

The current-voltage (*J-V*) characteristics of P3HT:PC$_{61}$BM:P3HT-*b*-PHIC blend solar cells were recorded under AM 1.5 AMG illumination. Figure 5 shows the cell data obtained for the blends with various contents of P3HT-*b*-PHIC. A summary of the averaged *J-V* characteristics is given in Table 3. The PCE for the P3HT:PC$_{61}$BM binary blend was 2.43 %. As shown in Figure 5 and Table 3, by adding 15 wt.% diblock copolymer, the PCE increased to 2.66 %. The ternary blend with 20 wt.% and 30 wt.% P3HT-*b*-PHIC diblock copolymer gave an overall reduction of PCE to 2.60% and 2.46%, respectively. The TMAFM analysis was performed on the active layer blends for the devices with 0 wt.%, 15 wt.%, and 30 wt.% P3HT-*b*-PHIC (Figure 6, Figure S9, Supporting Information). Average surface roughness (R.M.S) measured was 1.24 nm, 3.13 nm, and 6.55 nm for 0 wt.%, 15 wt.%, and 30 wt.% P3HT-*b*-PHIC, respectively.

The different roughness indicated that the morphology changed as a function of weight % of P3HT-*b*-PHIC added.

Table 3. Photovoltaic properties of devices with different percentage of P3HT-*b*-PHIC[a]

P3HT-*b*-PHIC (%)	V_{oc} (V)	J_{sc} (mA/cm^2)	FF (%)	PCE (%)	Thickness (nm)
0%	0.55	7.79 (7.99)	55%	2.43 (2.46)	246.2
15%	0.57	8.46 (8.80)	55%	2.66 (2.71)	231.5
20%	0.57	8.29 (8.58)	55%	2.60 (2.65)	229.5
30%	0.58	7.57 (7.62)	55%	2.46 (2.48)	215.3

[a]PC$_{61}$BM was used as acceptor.

[b]Data in the parenthesis represents the highest value (four devices were tested and the average values were determined)
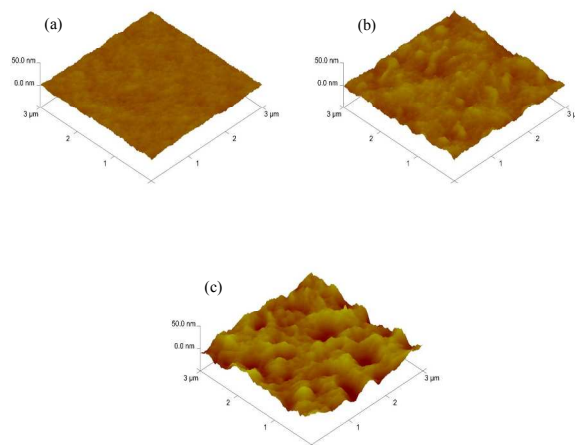

Figure 6. 3D TMAFM images of the solar cell devices with (a) 0% P3HT-*b*-PHIC (r.m.s=1.24 nm); (b) 15% P3HT-*b*-PHIC (r.m.s=3.13 nm); (c) 30% P3HT-*b*-PHIC (r.m.s=6.55 nm); scan size (3×3μm)

When 15 wt.% P3HT-*b*-PHIC was added, more phase separation in the active layer resulted, which most likely contributed to better charge transport.[54, 55] An increase in the J_{sc} (8.46 mA/cm^2) was obtained when 15 wt.% P3HT-*b*-PHIC was added as compared with the P3HT:PC$_{61}$BM device (7.79 mA/cm^2). However, when 30 wt.% P3HT-*b*-PHIC was added, the surface of the active layer became rougher and large isolated domains appeared as shown in Figure 6. A decrease of the J_{sc} to 7.57 mA/cm^2 was attributed to the rough surface and the presence large domains.

In order to confirm the effect of P3HT-*b*-PHIC, PC$_{71}$BM was also used as an acceptor for BHJ solar cells. The photovoltaic properties are summarized in Figure 7 and Table 4. An increase in the PCE from 2.57% to 2.83% was also observed when 15 wt.% P3HT-*b*-PHIC was added to the active layer blend. By varying the content of P3HT-*b*-PHIC, the PCE showed the same

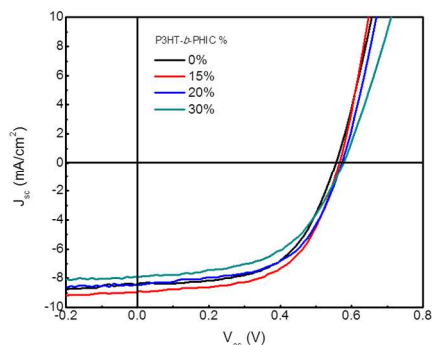trend as it was observed for $PC_{61}BM$ blends.

Figure 7. *J-V* curves for devices with different percentage of P3HT-*b*-PHIC

Table 4. Photovoltaic properties of devices with different percentage of P3HT-*b*-PHIC[a]

P3HT-*b*-PHIC (%)	V_{oc} (V)	J_{sc} (mA/cm^2)	FF (%)	PCE (%)	Thickness (nm)
0%	0.56	8.20 (8.37)	56%	2.57 (2.72)	244.6
15%	0.56	8.82 (8.91)	58%	2.83 (2.95)	219.6
20%	0.57	8.24 (8.44)	58%	2.72 (2.74)	218.6
30%	0.57	7.53 (7.90)	55%	2.36 (2.44)	206.2

[a]$PC_{71}BM$ was used as acceptor.

[b]Data in the parenthesis represents the highest value (four devices were tested and the average values were calculated)

For the binary blend P3HT:$PC_{71}BM$ device, a V_{oc} of 0.56 V, J_{sc} of 8.20 mA/cm^2, and FF of 56% were measured. For the ternary blend devices with 15 wt.% P3HT-*b*-PHIC, an increase in the J_{sc} to 8.82 mA/cm^2 was observed. The PCE decreased when the content of P3HT-*b*-PHIC was increased above 15 wt.%. The TMAFM images were obtained for devices with 0 wt.%, 15 wt.%, and 30 wt.% P3HT-*b*-PHIC. An increase of the average roughness from 2.59 nm to 5.01 nm upon addition of 15 wt.% P3HT-*b*-PHIC indicated that P3HT-*b*-PHIC affected the morphology of the active layer. Presumably a better phase separation for devices with 15 wt.% P3HT-*b*-PHIC improved the charge transport and thus resulted in the increase of the J_{sc} to 8.82 mA/cm^2. By contrast, the addition of 30 wt.% P3HT-*b*-PHIC in the blend created larger domains and presumably a less favourable morphology of the active layer blend. A J_{sc} of 7.53 mA/cm^2 was measured for the blend with 30 wt.% P3HT-*b*-PHIC, which is in agreement with the data obtained with $PC_{61}BM$ acceptor.

Liquid crystalline properties

The liquid crystalline properties of the diblock copolymer were investigated by polarizing microscope under cross-polarizer. The polarized optical micrograph of a concentrated solution of the

diblock copolymer in xylene (40 wt %), which was viewed at 10x magnification under crossed polarizers, is shown in Figure 9. The micrograph indicated that the PHIC in the diblock copolymer was predominant and thus the block copolymer solution retained the liquid crystalline properties of the PHIC.
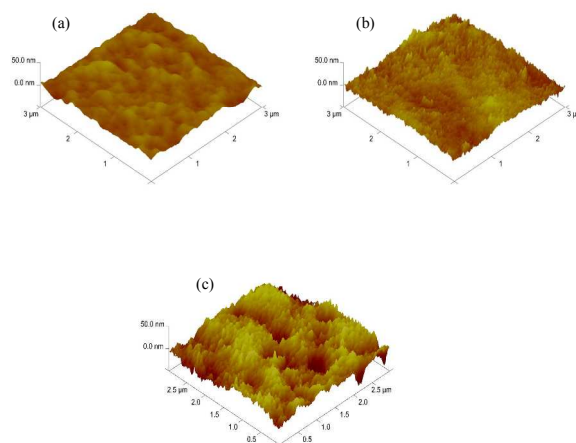

Figure 8. 3D TMAFM images of the solar cell devices with (a) 0% P3HT-*b*-PHIC (r.m.s=2.59 nm); (b) 15% P3HT-*b*-PHIC (r.m.s=5.01 nm); (c) 30% P3HT-*b*-PHIC (r.m.s=10.30 nm); scan size (3×3μm)
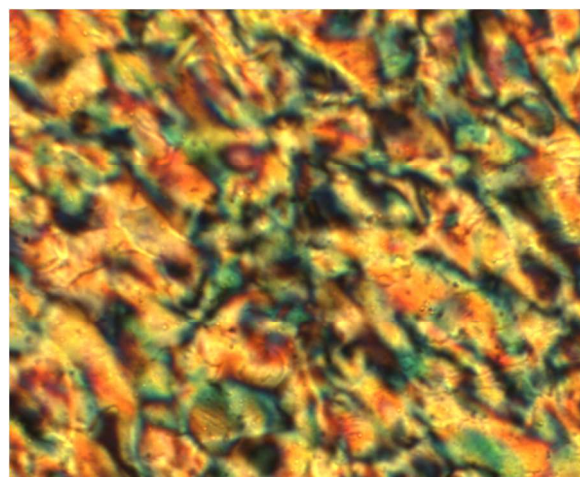

Figure 9. Optical micrograph of P3HT-*b*-PHIC; 40 wt% of polymer in xylene

X-Ray diffraction studies

Thin film XRD measurements were performed for the P3HT precursor, PHIC homopolymer (M_n = 13000 g mol^{-1}), and the P3HT-*b*-PHIC diblock copolymer films deposited from chloroform.

The XRD pattern obtained for the precursor P3HT indicated the presence of a peak at 2θ = 5.38° (d = 16.4 Å) corresponding to the (100) lamellar stacking of P3HT. The film also showed higher order reflections of the P3HT stacking (200) and (300) at 2θ = 10.87° and 2θ = 16.48° corresponding to d-spacings of 8.13 Å and 5.37 Å respectively (Figure 10 (a)).
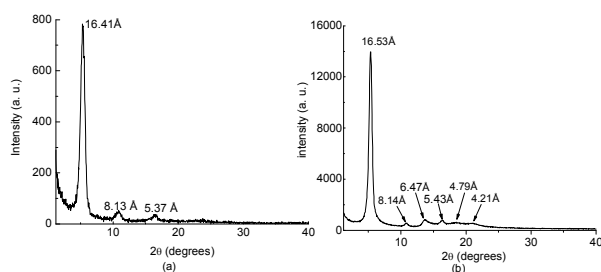
Figure 10. X-Ray diffraction patterns of (a) P3HT precursor and (b) P3HT-*b*-PHIC

These data are consistent with the data reported for the XRD of the P3HT homopolymer.[56] The XRD pattern obtained from the PHIC homopolymer thin film showed peaks at $2\theta = 5.41°$, $6.48°$, $13.55°$, and $16.84°$ corresponding the d-spacing of 16.32 Å, 13.63 Å, 6.53 Å, and 5.26 Å, respectively (Figure S11, Supporting Information). The P3HT-*b*-PHIC block copolymer displayed six characteristic peaks, indicating that the block copolymer self-assembled and preserved the crystallinity of its constituent blocks. While the peak corresponding to the first order lamellar stacking (100) of 16.53 Å may be not be concretely assigned to one block over the other, the higher order reflections reveal that the inherent ordering of the two individual blocks was maintained (Figure 10 (b)). The second ($2\theta = 10.86°$) and third ($2\theta = 16.30°$) order lamellar stacking with the d-spacing of ~8.1 Å and ~5.4 Å were clearly evident in the diffraction profiles for both the precursor P3HT (Figure 10 (a)) and the diblock copolymer (Figure 10 (b)). The XRD pattern also revealed the higher order reflection peaks of the PHIC block ($2\theta = 13.66°$), ($2\theta = 18.48°$), and ($2\theta = 21.07°$) corresponding to the d-spacing of 6.47 Å, 4.79 Å, and 4.21 Å, respectively. These results indicate that the diblock copolymer self-assembled in such a way that PHIC and P3HT domains demonstrate long range ordering comparable to that of the corresponding homopolymers.

Conclusions

A semiconducting diblock copolymer containing liquid crystalline segment was synthesized by the combination of GRIM and titanium mediated coordination polymerization methods. Electronic properties and liquid crystallinity of the copolymer were investigated and revealed. The block copolymer displayed a mesophase under cross polarized microscope and also showed promising results in OFETs. The TMAFM images of the block copolymer thin films displayed nanoscale morphology. The use of diblock copolymer as additive for P3HT/PCBM bulk heterojunction solar cells was investigated. Upon addition of 15% P3HT-*b*-PHIC to the photoactive layer, the PCE improved by about 9 %. X-ray diffraction pattern obtained for the block copolymer showed that the overall structural morphology is driven by the liquid crystalline block.

Notes and references

University of Texas at Dallas, Department of Chemistry, 800 West Campbell Road, Richardson, TX 75080, USA. Fax: 972-883-2925; Tel: 972-883-6581; E-mail: mihaela@utdallas.edu
†*Electronic Supplementary Information (ESI) available: ^{1}H NMR, XRD patterns, UV-Vis spectra and SEC traces. See DOI: 10.1039/b000000x/*

1. C. W. G. Fishwick, A. J. Beevers, L. M. Carrick, C. D. Whitehouse, A. Aggeli and N. Boden, *Nano. Lett.*, 2003, **3**, 1475-1479.
2. A. J. Bur and L. J. Fetters, *Chem. Rev.*, 1976, **76**, 727-746.
3. D. N. Rubingh and H. Yu, *Macromolecules*, 1976, **9**, 681-685.
4. O. Vogl and G. D. Jaycox, *Polymer*, 1987, **28**, 2179-2182.
5. G. Wulff, *Angew. Chem. Int. Edit.*, 1989, **28**, 21-37.
6. Y. Okamoto and T. Nakano, *Chem. Rev.*, 1994, **94**, 349-372.
7. M. M. Green, N. C. Peterson, T. Sato, A. Teramoto, R. Cook and S. Lifson, *Science*, 1995, **268**, 1860-1866.
8. S. Mayer and R. Zentel, *Prog. Polym. Sci.*, 2001, **26**, 1973-2013.
9. T. Norisuye, *Prog. Polym. Sci.*, 1993, **18**, 543-584.
10. S. M. Aharoni, *Macromolecules*, 1979, **12**, 94-103.
11. S. M. Aharoni, *Polymer*, 1980, **21**, 21-30.
12. K. Maeda and Y. Okamoto, *Macromolecules*, 1998, **31**, 5164-5166.
13. S. Lifson, C. E. Felder and M. M. Green, *Macromolecules*, 1992, **25**, 4142-4148.
14. A. E. Tonelli, *Macromolecules*, 1974, **7**, 628-631.
15. S. Allenmark, *Chirality*, 2003, **15**, 409-422.
16. T. C. Troxell and H. A. Scheraga, *Macromolecules*, 1971, **4**, 528-539.
17. T. Sato and A. Teramoto, *Adv. Polym. Sci.*, 1996, **126**, 85-161.
18. A. Sugita, Y. Yamashita and S. Tasaka, *J. Polym. Sci., Part B: Polym. Phys.*, 2005, **43**, 3093-3099.
19. J.-H. Ahn, Y.-D. Shin, S.-Y. Kim and J.-S. Lee, *Polymer*, 2003, **44**, 3847-3854.
20. M. Kikuchi, L. T. N. Lien, A. Narumi, Y. Jinbo, Y. Izumi, K. Nagai and S. Kawaguchi, *Macromolecules (Washington, DC, U. S.)*, 2008, **41**, 6564-6572.
21. G. Zorba, M. Pitsikalis and N. Hadjichristidis, *J. Polym. Sci., Part A: Polym. Chem.*, 2007, **45**, 2387-2399.
22. T. E. Patten and B. M. Novak, *J. Am. Chem. Soc.*, 1996, **118**, 1906-1916.
23. Y. Rho, J. Min, J. Yoon, B. Ahn, S. Jung, K. Kim, P. N. Shah, J.-S. Lee and M. Ree, *NPG Asia Mater*, 2012, **4**, e29.
24. S. M. Hoff and B. M. Novak, *Macromolecules*, 1993, **26**, 4067-4069.
25. Y. D. Shin, J. H. Ahn and J. S. Lee, *Polymer*, 2001, **42**, 7979-7985.
26. M. Kawaguchi, R. Ishikawa, T. Yamamoto, T. Kuki and T. Kato, *Langmuir*, 2001, **17**, 384-387.
27. I. K. Yang and A. D. Shine, *J. Rheol.*, 1992, **36**, 1079-1104.
28. T. J. Menna and F. E. Filisko, *J. Polym. Sci., Part B: Polym. Phys.*, 2005, **43**, 1124-1133.
29. K.-L. Tse and A. D. Shine, *Macromolecules*, 2000, **33**, 3134-3141.
30. M. Kawaguchi and M. Suzuki, *J. Colloid Interface Sci.*, 2005, **288**, 548-552.
31. M. Kawaguchi, M. Yamamoto, N. Kurauchi and T. Kato, *Langmuir*, 1999, **15**, 1388-1391.
32. T. A. Skotheim and J. Reynolds, *Handbook of Conducting Polymers*, CRC Press, LLC, Boca Raton, 2006.

33. I. F. Perepichka, D. F. Perepichka and Editors, *Handbook of Thiophene-based Materials: Applications in Organic Electronics and Photonics, Volume One: Synthesis and Theory*, 2009.

34. R. S. Loewe, S. M. Khersonsky and R. D. McCullough, *Adv. Mater.*, 1999, **11**, 250-253.

35. M. C. Iovu, E. E. Sheina, R. R. Gil and R. D. McCullough, *Macromolecules*, 2005, **38**, 8649-8656.

36. M. Jeffries-El, G. Sauve and R. D. McCullough, *Adv. Mater.*, 2004, **16**. 1017-1019.

37. M. Jeffries-El, G. Sauve and R. D. McCullough, *Macromolecules*, 2005, **38**, 10346-10352.

38. K. Palaniappan, N. Hundt, P. Sista, H. Nguyen, J. Hao, M. P. Bhatt, Y.-Y. Han, E. A. Schmiedel, E. E. Sheina, M. C. Biewer and M. C. Stefan, *J. Polym. Sci., Part A: Polym. Chem.*, 2011, **49**, 1802-1808.

39. M. C. Iovu, C. R. Craley, M. Jeffries-El, A. B. Krankowski, R. Zhang, T. Kowalewski and R. D. McCullough, *Macromolecules*, 2007, **40**, 4733-4735.

40. M. C. Stefan, M. P. Bhatt, P. Sista and H. D. Magurudeniya, *Polym. Chem.*, 2012, **3**, 1693-1701.

41. G. W. Heffner and D. S. Pearson, *Macromolecules*, 1991, **24**, 6295-6299.

42. M. P. Bhatt, P. Sista, J. Hao, N. Hundt, M. C. Biewer and M. C. Stefan, *Langmuir*, 2012, **28**, 12762-12770.

43. Z.-Q. Wu, R. J. Ono, Z. Chen, Z. Li and C. W. Bielawski, *Polym. Chem.*, 2011, **2**, 300-302.

44. N. Hundt, Q. Hoang, H. Nguyen, P. Sista, J. Hao, J. Servello, K. Palaniappan, M. Alemseghed, M. C. Biewer and M. C. Stefan, *Macromol. Rapid Commun.*, 2011, **32**, 302-308.

45. X. Chen, L. Chen, K. Yao and Y. Chen, *ACS Appl. Mater. Interfaces.*, 2013, **5**, 8321-8328.

46. M. G. Alemseghed, S. Gowrisanker, J. Servello and M. C. Stefan, *Macromol. Chem. Phys.*, 2009, **210**, 2007-2014.

47. M. G. Alemseghed, J. Servello, N. Hundt, P. Sista, M. C. Biewer and M. C. Stefan, *Macromol. Chem. Phys.*, 2010, **211**, 1291-1297.

48. X. Yu, K. Xiao, J. Chen, N. V. Lavrik, K. Hong, B. G. Sumpter and D. B. Geohegan, *ACS Nano*, 2011, **5**, 3559-3567.

49. Y.-K. Fang, C.-L. Liu, C. Li, C.-J. Lin, R. Mezzenga and W.-C. Chen, *Adv. Funct. Mater.*, 2010, **20**, 3012-3024.

50. M. C. Iovu, R. Zhang, J. R. Cooper, D. M. Smilgies, A. E. Javier, E. E. Sheina, T. Kowalewski and R. D. McCullough, *Macromol. Rapid Commun.*, 2007, **28**, 1816-1824.

51. M. P. Bhatt, M. K. Huynh, P. Sista, H. Q. Nguyen and M. C. Stefan, *J. Polym. Sci., Part A: Polym. Chem.*, 2012, **50**, 3086-3094.

52. M. C. Iovu, M. Jeffries-El, R. Zhang, T. Kowalewski and R. D. McCullough, *J. Macromol. Sci., Part A: Pure Appl. Chem.*, 2006, **43**, 1991-2000.

53. C. Yang, J. K. Lee, A. J. Heeger and F. Wudl, *J. Mater. Chem.*, 2009, **19**, 5416-5423.

54. J. M. Lobez, T. L. Andrew, V. Bulovic and T. M. Swager, *ACS Nano*, **6**, 3044-3056.

55. J.-H. Tsai, Y.-C. Lai, T. Higashihara, C.-J. Lin, M. Ueda and W.-C. Chen, *Macromolecules*, 2010, **43**, 6085-6091.

56. M. Kobashi and H. Takeuchi, *Macromolecules*, 1998, **31**, 7273-7278.